

Optimal two-qubit gates in recurrence protocols of entanglement purification

Francesco Preti,^{1,2} Tommaso Calarco,^{1,2} Juan Mauricio Torres,³ and József Zsolt Bernád¹

¹*Peter Grünberg Institute (PGI-8), Forschungszentrum Jülich, D-52425 Jülich, Germany*

²*Institute for Theoretical Physics, University of Cologne, D-50937 Cologne, Germany**

³*Instituto de Física, Benemérita Universidad Autónoma de Puebla, Apartado Postal J-48, Puebla 72570, Mexico*

(Dated: May 25, 2022)

We propose and investigate a method to optimize recurrence entanglement purification protocols. The approach is based on a numerical search in the whole set of $SU(4)$ matrices with the aid of a quasi-Newton algorithm. Our method evaluates average concurrences where the probabilistic occurrence of noisy entangled states is also taken into account. We show for certain families of states that optimal protocols are not necessarily achieved by bilaterally applied controlled-NOT gates. As we discover several optimal solutions, the proposed method offers some flexibility in experimental implementations of entanglement purification protocols and interesting perspectives in quantum information processing.

I. INTRODUCTION

Entanglement is a key resource for quantum information tasks, like quantum simulations [1], computation [2], and communication [3]. These tasks are based on the idea of creating networks of quantum systems, where the generation of well-controlled entanglement between spatially separated nodes is essential. These networks, which may consist of distant or nearby nodes, have been thoroughly investigated for efficient process and transfer of quantum information [4]. However, due to interactions with an uncontrollable environment noisy or non-maximally entangled states are produced. To protect quantum information and to guarantee a high performance of its processing, one can use quantum error correction [5, 6] or quantum teleportation in combination with entanglement purification [7–9]. Quantum error correction is particularly suitable for quantum computers, however it is inferior to entanglement purification with two-way classical communication [9], which is the subject of our investigations. In particular, we consider a so-called recurrence protocol [10], an iterative approach, which operates in each purification step only on two identical copies of states.

In this paper, we discuss entanglement purification from the point of view of optimality. Recently, optimized entanglement purification has been investigated with the help of genetic algorithms [11], where the analytical and numerical studies are based on Werner states [12]. In fact, also the first ever proposed protocols are based on either Werner [7] or Bell diagonal states [8]. It has been shown that 4 or 12 local random $SU(2)$ transformations can bring any states into a Bell diagonal or Werner state, respectively [9]. We have already argued that these random local unitary transformations and states obtained in consequence are only useful for grasping and consequently understanding the complex task of purification because they may waste useful entanglement [13]. There-

fore, here, we develop a method for general states and demonstrate it for several simple examples including also the Werner state. Nonetheless, our motivation also lies in the fact that an experimental implementation may not have enough control over the generated noisy states and thus more general, adaptive, and optimal purification strategies have to be made available. In this general context, we assume that an experiment can still guarantee identical copies of states before the purification protocol takes place.

Our method is based on quasi-Monte Carlo numerical sampling of the states, which undergo the purification protocol, and then the concurrence [14] of the output states is integrated over an *a priori* probability distribution function. This results in an average two-qubit gate-dependent cost function for the whole sample of states and then we employ a quasi-Newton algorithm [15] for solving this non-linear optimization problem on the whole $SU(4)$ group. The obtained two-qubit gate is optimal in the sense that it achieves, on average, a higher increase of entanglement of an input family of states. We discuss the performance of our method for several examples and compare with protocols based on one bilateral application of controlled-NOT gates, the paradigmatic two-qubit operation used in the seminal purification protocols [7, 8].

The paper is organized as follows. In Sec. II we introduce our method and give some elementary examples to allow further acquaintance with the concept of the introduced cost function. In Sec. III we demonstrate our approach for four one-parameter and one two-parameter family of states. Numerical and analytical results are presented for concurrences and success probabilities. In Sec. IV we summarize and draw our conclusions. Some details supporting the main text are collected in Appendix A.

II. METHOD

In this section, we describe how the recurrence protocol is optimized with respect to an input family of quantum

* f.preti@fz-juelich.de

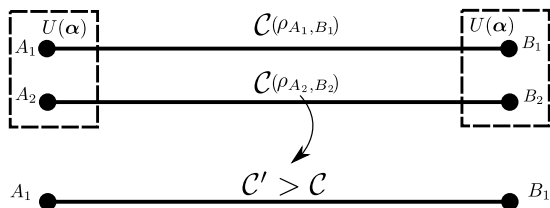


FIG. 1: Schematic representation of bipartite entanglement purification, where the entanglement purification protocol trades two entangled qubit pairs for a qubit pair with a higher degree of entanglement, which is quantified by the concurrence \mathcal{C} .

states.

A. Entanglement purification protocol

Let us consider the product state of two-qubit pairs

$$\rho = \rho^{A_1, B_1} \otimes \rho^{A_2, B_2}, \quad (1)$$

where qubit components of each pair are assumed to be spatially separated at distant locations. These locations are labeled by A and B . In an entanglement purification protocol, one performs local quantum operations, which may not just involve two-qubit gates [16]. This is followed by measurements on one of the pairs at both locations. A classical communication between A and B results in a qubit pair with a higher degree of entanglement. Both pairs are assumed to start in the same state ρ and the degree of the entanglement is usually measured by the fidelity with respect to one of the Bell states

$$|\Psi^\pm\rangle = \frac{1}{\sqrt{2}} (|01\rangle \pm |10\rangle), \quad |\Phi^\pm\rangle = \frac{1}{\sqrt{2}} (|00\rangle \pm |11\rangle). \quad (2)$$

However, these states can be subject to local unitary transformations, which can cause some technical difficulties, when one uses fidelity, i.e. using fidelity as a cost function would force us to search also for additional local unitary operations in order to align the output state of the protocol with the Bell basis. As we intend to analyze the entanglement purification in a very general setup, one requires an entanglement measure that is invariant under local unitary transformations. Therefore, we turn to the concurrence as a measure of the attainability of a maximally entangled state [14]:

$$\mathcal{C}(\rho) = \max\{0, \lambda_1 - \lambda_2 - \lambda_3 - \lambda_4\}. \quad (3)$$

Here $\lambda_1, \lambda_2, \lambda_3, \lambda_4$ are the square roots of the non-negative eigenvalues of the non-Hermitian matrix

$$\tilde{\rho} = \rho(\sigma_y \otimes \sigma_y) \rho^* (\sigma_y \otimes \sigma_y),$$

with $*$ being the complex conjugation in the standard basis and σ_y is the Pauli matrix.

In this manuscript, we examine and optimize a

purification protocol having the following steps:

(I) Two unitary transformations $\rho \rightarrow U(\alpha)\rho U(\alpha)^\dagger$ are applied locally at A and B (see Fig. 1), where U is a general two-qubit unitary described by a parameter vector α . After the application of the quantum operation the four-qubit system attains the state

$$\rho' = U_{A_1, A_2}(\alpha) U_{B_1, B_2}(\alpha) \rho U_{B_1, B_2}^\dagger(\alpha) U_{A_1, A_2}^\dagger(\alpha). \quad (4)$$

(II) One of the pairs (A_2, B_2) is then locally measured in the standard basis. There are four possible states, i.e., 4-dimensional vectors, in which one can find the measured pair:

$$\begin{aligned} |1\rangle &= |00\rangle_{A_2, B_2}, & |2\rangle &= |01\rangle_{A_2, B_2}, \\ |3\rangle &= |10\rangle_{A_2, B_2}, & |4\rangle &= |11\rangle_{A_2, B_2}. \end{aligned}$$

A successful measurement of one of the states $|i\rangle$ with $i \in \{1, 2, 3, 4\}$ results in a state for the other qubit

$$\tilde{\rho}'_i = \frac{\langle i | \rho' | i \rangle}{\text{Tr}\{\langle i | \rho' | i \rangle\}} \quad (5)$$

with probability

$$p_i = \text{Tr}\{\langle i | \rho' | i \rangle\}.$$

(III) Depending on value of the measurement results, which are communicated between the two parties, the state with largest concurrence and the related success probability are kept, whereas the others are discarded. The output of the protocol is the pair (\mathcal{C}', P) , concurrence value \mathcal{C}' of the state obtained with probability P . If there are multiple maxima, e.g., $\mathcal{C}(\tilde{\rho}'_1) = \mathcal{C}(\tilde{\rho}'_2)$, then $\mathcal{C}' = \mathcal{C}(\tilde{\rho}'_1)$ and $P = p_1 + p_2$.

Given two copies of a state ρ with concurrence \mathcal{C} , it is straightforward to see that pair (\mathcal{C}', P) depends on the vector α , which we use as the optimization parameter.

Recurrence entanglement purification protocols might include symmetric and asymmetric single-qubit gates before and after the bilateral action of the two-qubit operations [7, 8]. These are important in an analytical approach to maintain the form of the state after each iteration, however, entanglement is not affected by this process. In this work, we shall omit these single-qubit gates as we are focused on increasing the value of the concurrence and not on the specific form of the state after each iteration step.

B. Protocol optimization

In order to optimize the protocol described in Sec. II A, we first define an appropriate parametrization for the two-qubit unitary operations used in Eq. (4). In principle, one should consider elements from $U(4)$, the group of 4×4 unitary matrices, which contains the subgroup

$SU(4)$. However, $U(4)$ is the semi-direct product of $U(1)$ and $SU(4)$, where elements of $U(1)$ are rotations of the unit circle [17]. Therefore, choosing elements from $SU(4)$ in Eq. (4) represents the most general unitary quantum operation involving two-qubit gates at locations A and B . Elements in $SU(4)$ can be parametrized in the following way [18]:

$$U(\boldsymbol{\alpha}) = e^{i\sigma_3\alpha_1} e^{i\sigma_2\alpha_2} e^{i\sigma_3\alpha_3} e^{i\sigma_5\alpha_4} e^{i\sigma_3\alpha_5} e^{i\sigma_{10}\alpha_6} e^{i\sigma_3\alpha_7} e^{i\sigma_2\alpha_8} e^{i\sigma_3\alpha_9} e^{i\sigma_5\alpha_{10}} e^{i\sigma_3\alpha_{11}} e^{i\sigma_2\alpha_{12}} e^{i\sigma_3\alpha_{13}} e^{i\sigma_8\alpha_{14}} e^{i\sigma_{15}\alpha_{15}},$$

with $\boldsymbol{\alpha} = (\alpha_1, \alpha_2, \dots, \alpha_{15})^T \in \mathbb{R}^{15}$ (T denotes the transposition), and

$$\begin{aligned} 0 &\leq \alpha_1, \alpha_3, \alpha_5, \alpha_7, \alpha_9, \alpha_{11}, \alpha_{13} \leq \pi, \\ 0 &\leq \alpha_2, \alpha_4, \alpha_6, \alpha_8, \alpha_{10}, \alpha_{12} \leq \frac{\pi}{2} \\ 0 &\leq \alpha_{14} \leq \frac{\pi}{\sqrt{3}}, \quad 0 \leq \alpha_{15} \leq \frac{\pi}{\sqrt{6}}, \end{aligned} \quad (6)$$

where σ_i , $i = 1, \dots, 15$ form a Gell-Mann type basis of the Lie group $SU(4)$, see Appendix A. This is called the Euler angle parametrization of $SU(4)$, which is sufficient to represent every element of the Lie group. For example, the canonical parametrization e^{iH} , where H is a 4×4 self-adjoint matrix with trace zero, is not minimal, because after exponentiation we may have multiple wrappings around the great circles of the 7-sphere.

Our aim is to increase the concurrence, which is a non-linear function of the state ρ and the protocol's unitary matrix U . Furthermore, we have lower and upper bounds on $\boldsymbol{\alpha}$, as given in Eq. (6). We then consider a cost function $f: \mathbb{R}^{15} \rightarrow \mathbb{R}$ as

$$f(\boldsymbol{\alpha}) = 1 - \mathcal{C}'(\boldsymbol{\alpha}) \quad (7)$$

and our optimization problem is, to find local minimizers, e.g., a point $\boldsymbol{\alpha}^*$ such that

$$f(\boldsymbol{\alpha}^*) \leq f(\boldsymbol{\alpha})$$

for all $\boldsymbol{\alpha}$ in the Euclidean norm defined neighborhood of $\boldsymbol{\alpha}^*$. The gradient $\nabla f(\boldsymbol{\alpha})$ can be made available to us due to an automatic differentiation [19], so we implement for the optimization a quasi-Newton algorithm the so-called limited memory Broyden-Fletcher-Goldfarb-Shanno (L-BFGS) method [20]. Here, we have a constrained optimization problem, because $\boldsymbol{\alpha}$ takes values in the hyperrectangle defined by Eq. (6) and thus we use the L-BFGS approach of Ref. [21]. As long as the state to be purified is given, the above approach yields an optimal $\boldsymbol{\alpha}^*$ and a concurrence \mathcal{C}' as close as possible to one. The vector $\boldsymbol{\alpha}^*$ gives the best two-qubit unitary gate associated with this given state. However, our main aim is to provide the best gate, which is capable to purify most effectively certain class of states and not only a fixed one. This is relevant in a scenario where the generation of distant entanglement is affected by noise, leading to slightly different types of states entering the protocol. In order to formulate this quantitatively we introduce a probability

density function (PDF) $p(\mathbf{x})$, where the vector \mathbf{x} defines uniquely the state ρ according to a parametrization. For example, in the case of a Werner state [12]

$$\begin{aligned} \hat{\rho}(x) = & x|\Psi^-\rangle\langle\Psi^-| + \frac{1-x}{3}|\Psi^+\rangle\langle\Psi^+| \\ & + \frac{1-x}{3}|\Phi^-\rangle\langle\Phi^-| + \frac{1-x}{3}|\Phi^+\rangle\langle\Phi^+|, \end{aligned} \quad (8)$$

we have $x \in [0, 1]$ and the PDF satisfies

$$\int_0^1 p(x) dx = 1.$$

In general, a two-qubit state can be described by 15 parameters, which have to fulfill some non-trivial conditions [22–24]. The choice of the PDF is not straightforward and the only guideline we have is that the support $\text{supp}(p)$ consists of all \mathbf{x} , which define entangled states. This is motivated by the fact that separable states are not purifiable. In the case of the Werner states, the support of the PDF is the interval $(0.5, 1]$. Thus, the PDF may put more weight on states with a given concurrence.

Algorithm 1 Optimization of recurrence protocol

Input $\rho(\mathbf{x})$, optimizer OPT

Output $\rho(\mathbf{x})$

```

1: for  $j = 1$  to  $M$  do
2:    $\mathbf{x}_j \sim p(\mathbf{x}_j)$ 
3:    $\rho_j = \rho(\mathbf{x}_j)$ 
4: end for
5: for  $i = 1$  to  $N$  do
6:    $U_{AB}(\boldsymbol{\alpha}) = U_{A1,A2}(\boldsymbol{\alpha})U_{B1,B2}(\boldsymbol{\alpha})$ 
7:   for  $j = 1$  to  $M$  do
8:      $\sigma^j(\boldsymbol{\alpha}) = U_{AB}(\boldsymbol{\alpha})\rho_j U_{AB}^\dagger(\boldsymbol{\alpha})$ 
9:     for  $l = 1$  to 4 do
10:       $\sigma_A^{jl}(\boldsymbol{\alpha}) = \frac{\langle l | \sigma^j(\boldsymbol{\alpha}) | l \rangle}{\text{Tr}\{|l\rangle\langle l | \sigma^j(\boldsymbol{\alpha})\}}$ 
11:    end for
12:   end for
13:    $\mathcal{C}^l(\boldsymbol{\alpha}) = \frac{1}{M} \sum_{j=1}^M \mathcal{C}(\sigma_A^{jl})$ 
14:    $l' = \underset{l=1,2,3,4}{\text{argmin}} (1 - \mathcal{C}^l(\boldsymbol{\alpha}))$ 
15:    $\bar{f}(\boldsymbol{\alpha}) = 1 - \mathcal{C}^{l'}(\boldsymbol{\alpha})$ 
16:    $\boldsymbol{\alpha}^* = \text{OPT}(\bar{f}(\boldsymbol{\alpha}), \nabla_{\boldsymbol{\alpha}} \bar{f}(\boldsymbol{\alpha}))$ 
17:    $\rho_j = \sigma_A^{j l'}(\boldsymbol{\alpha}^*) \otimes \sigma_A^{j l'}(\boldsymbol{\alpha}^*)$ 
18: end for

```

In this context, we have an output concurrence $\mathcal{C}'(\boldsymbol{\alpha}, \mathbf{x})$ depending on both the two-qubit gate and the input state. Therefore, we are going to use an average cost function

$$\bar{f}(\boldsymbol{\alpha}) = 1 - \int_{\text{supp}(p)} \mathcal{C}'(\boldsymbol{\alpha}, \mathbf{x}) p(\mathbf{x}) d\mathbf{x}, \quad (9)$$

in the L-BFGS algorithm. The integral can be either solved numerically or approximated via a quasi-Monte Carlo approach by sampling \mathbf{x} over its corresponding parameter distribution $p(\mathbf{x})$:

$$\bar{f}(\boldsymbol{\alpha}) = 1 - \mathbb{E}_{\mathbf{x} \sim p(\mathbf{x})} [\mathcal{C}'(\boldsymbol{\alpha}, \mathbf{x})]. \quad (10)$$

We chose the second approach since it proved to be precise enough and numerically faster. A summarize of the optimization routine can be seen in Algorithm 1.

Now, we shed light on the meaning of the average cost function through the following two examples. We employ the CNOT gate

$$U_{\text{CNOT}} = \begin{pmatrix} 1 & 0 & 0 & 0 \\ 0 & 1 & 0 & 0 \\ 0 & 0 & 0 & 1 \\ 0 & 0 & 1 & 0 \end{pmatrix} = e^{i\frac{3\pi}{4}} \times \underbrace{U'}_{\in SU(4)},$$

where U' in the Euler angle parametrization is given by setting

$$\begin{aligned} \alpha_3 &= \alpha_5 = \alpha_7 = \frac{\pi}{4}, \\ \alpha_4 &= \alpha_6 = \alpha_{10} = \frac{\pi}{2}, \end{aligned}$$

and the remaining 9 angles to zero in Eq. (6). By fixing the vector $\boldsymbol{\alpha}$, one is able to get a value for the average cost function of the CNOT gate and thus to evaluate its performance.

Example 1. Let us consider the state

$$\frac{1}{6} \begin{pmatrix} 1+2x & 0 & 0 & 1-4x \\ 0 & 2-2x & 0 & 0 \\ 0 & 0 & 2-2x & 0 \\ 1-4x & 0 & 0 & 1+2x \end{pmatrix}, \quad \text{with } x \in [0, 1] \quad (11)$$

subject to the purification protocol with CNOT gates. This state is a rotated Werner state and its concurrence reads

$$\mathcal{C}(x) = \begin{cases} 2x - 1 & x \in (0.5, 1], \\ 0 & x \in [0, 0.5]. \end{cases}$$

In fact, this example is based on the pioneering protocol of Ref. [25]. The output reads

$$\mathcal{C}'_{\text{CNOT}}(x) = \frac{3(4x^2 - 1)}{5 - 4x + 8x^2}, \quad \text{for } x \in (0.5, 1],$$

with success probability

$$P_{\text{CNOT}} = \frac{5 - 4x + 8x^2}{9}.$$

For the sake of simplicity, we consider a uniform PDF $p(x)$ with $\text{supp}(p) = (0.5, 1]$. Hence, the input average

cost function reads

$$\bar{f}_{\text{input}} = 1 - \int_{0.5}^1 \mathcal{C}(x)p(x) dx = 0.5,$$

and the application of the purification protocol with CNOT gates yields

$$\bar{f}_{\text{CNOT}} = 1 - \int_{0.5}^1 \mathcal{C}'(x)p(x) dx = 0.450103.$$

The result shows that the protocol with two identical copies of states allows one to increase on average the entanglement of the output states.

Example 2. Now, we consider the state

$$\begin{pmatrix} \frac{x}{2} & 0 & 0 & -\frac{x}{2} \\ 0 & 0 & 0 & 0 \\ 0 & 0 & 1-x & 0 \\ -\frac{x}{2} & 0 & 0 & \frac{x}{2} \end{pmatrix}, \quad \text{with } x \in [0, 1]. \quad (12)$$

This state with concurrence $\mathcal{C}(x) = x$ is perfectly purifiable in just one iteration of the protocol [13]. Hence,

$$\mathcal{C}'_{\text{CNOT}}(x) = 1,$$

with success probability

$$P_{\text{CNOT}} = \frac{x^2}{2}.$$

It is immediate from Eq. (9) that for *any* PDF with $\text{supp}(p) = [0, 1]$

$$\bar{f}_{\text{CNOT}} = 1 - \int_0^1 \mathcal{C}'(x)p(x) dx = 0.$$

This means that the CNOT gate is optimal for this family of states.

Example 3. As a last example, let us consider the initial state

$$x|\Phi^+\rangle\langle\Phi^+| + (1-x)|\Phi^-\rangle\langle\Phi^-|, \quad \text{with } x \in [0, 1], \quad (13)$$

and concurrence $\mathcal{C}(x) = |1 - 2x|$. After one iteration of the purification protocol with bilaterally applied CNOT gates, it is not hard to realize that the resulting state has the concurrence

$$\mathcal{C}'_{\text{CNOT}}(x) = (1 - 2x)^2$$

with success probability $P_{\text{CNOT}} = 1$. The output concurrence $\mathcal{C}'_{\text{CNOT}}(x)$ is less than or equal to $\mathcal{C}(x)$ for all $x \in [0, 1]$. Thus, we conclude by using the properties of concurrence and integration that

$$\int_0^1 \mathcal{C}'_{\text{CNOT}}(x)p(x) dx \leq \int_0^1 \mathcal{C}(x)p(x) dx \quad (14)$$

for *any* PDF with $\text{supp}(p) = [0, 1]$. Hence, the initial average cost function \bar{f}_{input} is always less than or equal to \bar{f}_{CNOT} . This is an example where the purification fails with the sole implementation of the CNOT gate. It must be noted that for $x \neq 0.5$, the state in this example can be purified with previous protocols [7, 8] that work on the Bell basis, and where the implementation with the CNOT gate is now accompanied by local single-qubit gates.

These examples demonstrate the meaning of the average cost function. It is obvious that a two-qubit gate can be optimal for certain family of states and less optimal for other type of state. In the subsequent section, we will investigate numerically several cases.

III. RESULTS

In this section it is demonstrated how our proposed method can find optimal purification schemes. Our first case is the continuation of *Example 1.* in Sec. II. We have seen so far that the CNOT gate in $N = 1$ purification round can reduce the average cost function \bar{f} approximately by 0.05. The simulation results with the input state in Eq. (11) show that the optimal $SU(4)$ gate for $N = 1$ has a similar improvement on \bar{f} as the CNOT gate, see Fig. 2. The optimal gates found for $N = 2$ and 3 can further reduce \bar{f} , however, it is easy to check that the CNOT gate is not optimal anymore for these rounds of iterations. In Fig. 2 it is also shown that a higher number of iterations result in more concave shapes of the corresponding concurrences. It is worth noting that the success probability of the second iteration is lower than the success probability of the first iteration. The overall success probability of 3 iterations, shown also in Fig. 2, is defined as: in the first iteration 4 qubit pairs, in the second iteration 2 qubit pairs, and in the third iteration the final qubit pair are successfully purified. These results show that states close to maximally entangled states can be produced already in the third iteration, but the overall success probability of the procedure is getting smaller with the number of iterations. The only fixed point is $\mathcal{C} = 1$. Thus our method seems to provide the same results to the one found in [25], which is based completely on the CNOT gate. As a result, we have investigated the circumstances where the CNOT gate is also optimal. It turns out that the local unitary transformation introduced by [8] and given by

$$b_{A_1}^\dagger \otimes b_{A_2}^\dagger \otimes b_{B_1} \otimes b_{B_2}, \quad (15)$$

where

$$b = \frac{\mathbb{I}_2 + i\sigma_x}{\sqrt{2}}$$

with the Pauli matrix σ_x and the identity map \mathbb{I}_2 , is crucial for the CNOT gate. This is the transformation, which transforms a Werner state in Eq. (8) into the state in Eq. (11). Now, if one applies Eq. (15) before all itera-

tions of the protocol involving only the CNOT gate, then the same curves are obtained as in Fig. 2. This means that there are more optimal protocols, which yield the same results, and our approach can find them. Thus, the analytically tractable CNOT-based protocol can be used as a benchmark to test the numerical accuracy of our method. Our numerics show at least a 2 decimal accuracy until the third iteration, but up to the fourth iteration, there is a breakdown in the numerical accuracy.

The one-parameter family of states in Eq. (11) has the same concurrence as the Werner state. Therefore, we consider the Werner state to be our next application. In Fig. 3 numerical results are presented for the average cost function \bar{f} and the overall success probability which exhibit the same behavior found for the one-parameter family of states in Eq. (11). In this case, one can note an improvement of 0.04 in \bar{f} after $N = 3$ iterations. This is less than the previously obtained value of 0.09 shown in Fig. 2. Furthermore, this is accompanied by another numerical inaccuracy: the overall success probability at $\mathcal{C} = 1$ is less than one. Given these results, the proposed method can find optimal entangling two-qubit gates for at least two iterations. It is also clear from these tests that the algorithm is always reducing \bar{f} , but from $N = 3$ iterations this might be not an optimal improvement of the concurrence. This originates from the fact that the gradient $\nabla f(\alpha)$, see Eq. (7), is almost flat in the neighborhood of $\mathcal{C} = 1$ for $N > 2$ iterations and thus the numerical search for the optimal gate, i.e, the search for $\alpha^* \in \mathbb{R}^{15}$, becomes inefficient.

Inspired by *Example 2.*, we consider the state in Eq. (12) and also

$$x|\Psi^-\rangle\langle\Psi^-| + (1-x)|\Upsilon\rangle\langle\Upsilon| \quad (16)$$

with $x \in [0, 1]$ and

$$|\Upsilon\rangle = \frac{1}{\sqrt{2}} (|\Psi^+\rangle + i|\Phi^-\rangle).$$

By using the unitary transformation in Eq. (15) on Eq. (16) one obtains Eq. (12) and therefore it is expected that the only optimal two-qubit gates are the ones that purify these states in one iteration. Both states have an input concurrence $\mathcal{C}(x) = x$. However, it is important to note that the CNOT gate is not optimal for the state in Eq. (16), because after one iteration round

$$\mathcal{C}'_{\text{CNOT}}(x) = \begin{cases} 0 & x \in [0, 0.5], \\ 2x\frac{2x-1}{1+x^2} & x \in (0.5, 1], \end{cases}$$

and $\mathcal{C}'_{\text{CNOT}}(x) \leq x$. The success probability is

$$P_{\text{CNOT}} = \frac{1+x^2}{2}.$$

Thus, the CNOT gate based purification protocol impairs the concurrence. In contrast to this analytical observation, numerical analysis with uniform PDF yields already

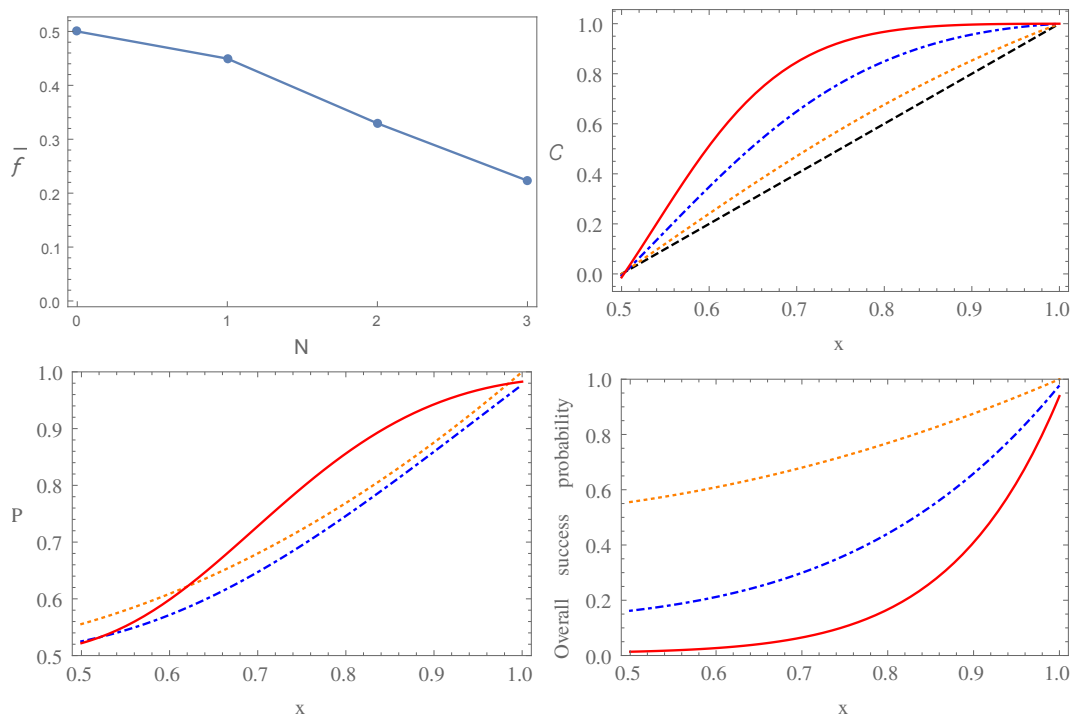


FIG. 2: Optimized purification protocol for the family of states in Eq. (11). Top left panel: average cost function \bar{f} with a uniform PDF as a function of N , the number of iterations. Top right panel: The concurrence C as a function of x . Four curves are presented for different values of iterations N : 0 or the input concurrence (dashed line), 1 (dotted line), 2 (dash-dotted line), and 3 (full line). Bottom left panel: Success probabilities as a function of x for different values of iterations N : 1 (dotted line), 2 (dash-dotted line), and 3 (full line). Bottom right panel: The overall success probability after $N = 1$ (dotted line), $N = 2$ (dash-dotted line), and $N = 3$ (full line) iterations as a function of x .

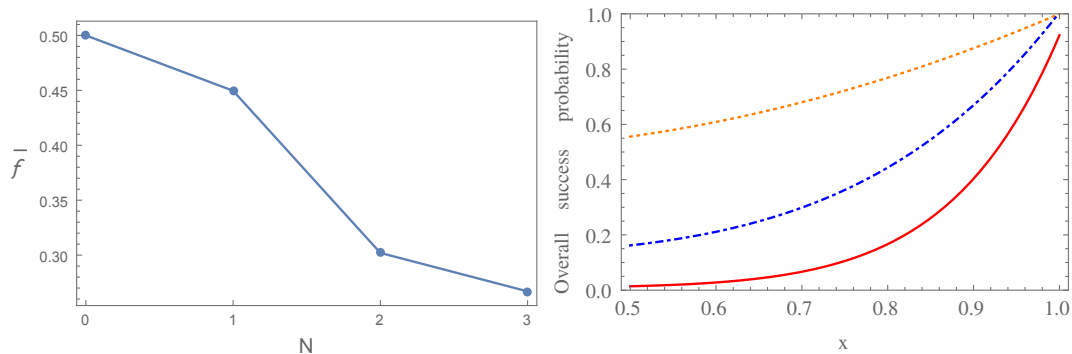


FIG. 3: Optimized purification protocol for Werner states, see Eq. (8). Left panel: average cost function \bar{f} with a uniform PDF as a function of N , the number of iterations. Right panel: The overall success probability after $N = 1$ (dotted line), $N = 2$ (dash-dotted line), and $N = 3$ (full line) iterations as a function of x .

in the first iteration for both states an average cost function $\bar{f} \approx 0.0002$. To demonstrate the robustness of the numerical approach we provide examples of three non-uniform PDFs for $N = 1$ iteration. First, we consider

$$p(x) = 2x, \quad \text{with } x \in [0, 1],$$

which describes a situation, where states with higher concurrences are more likely to be subject to the purification. The resulting average cost function is $\bar{f} \approx 0.000004$. Secondly, we take

$$p(x) = 2(1 - x), \quad \text{with } x \in [0, 1],$$

which puts more weight on states with low concurrences and find $\bar{f} \approx 0.0005$. Finally, we investigate a PDF

$$p(x) = 6x(1-x), \quad \text{with } x \in [0, 1],$$

i.e., the states around the concurrence $\mathcal{C}(x) = 0.5$ are more likely to participate in the purification, and obtain $\bar{f} \approx 0.00005$. These results demonstrate the effectiveness of our approach and up to a numerical precision these one-parameter families of states can be purified in one iteration.

Next, we consider the following two-parameter family of states [26]

$$\hat{\rho}(x, y) = \frac{1}{4} \begin{pmatrix} 1-x & iy & -iy & x-1 \\ -iy & x+1 & -x-1 & iy \\ iy & -x-1 & x+1 & -iy \\ x-1 & -iy & iy & 1-x \end{pmatrix} \quad (17)$$

with $x, y \in \mathbb{R}$ and $x^2 + y^2 \leq 1$. The concurrence of this state is $\sqrt{x^2 + y^2}$. In order to relate the performance of our approach, we apply the CNOT gate based purification protocol to this family of states. One obtains

$$\mathcal{C}'_{\text{CNOT}}(x, y) = \frac{2|x|}{1+x^2}, \quad (18)$$

$$P_{\text{CNOT}} = \frac{1+x^2}{2}, \quad (19)$$

after $N = 1$ and

$$\mathcal{C}'_{\text{CNOT}}(x, y) = \frac{4|x|(1+x^2)}{1+6x^2+x^4}, \quad (20)$$

$$P_{\text{CNOT}} = \frac{1+6x^2+x^4}{2(1+x^2)^2}, \quad (21)$$

after $N = 2$ purification rounds, respectively. If one applies the unitary transformation in Eq. (15) on the state before the bilateral CNOT gates are performed, then the above results remain unchanged. These results demonstrate that the CNOT gate and the additional tricks, which yielded optimal purifications for the one-parameter family of states, are not optimal in this scenario, since they are outperformed on average by our optimized protocol. We assume that CNOT-based purification protocols cannot exploit all the useful entanglement, because the concurrence and the success probability become independent of the y variable. Using these analytical results and the uniform PDF

$$p(x, y) = \frac{1}{\pi}, \quad \text{with } x^2 + y^2 \leq 1,$$

we compare our approach with the above-presented analytical results, see Eq. (18) and Eq. (20). In Fig. 4, we show that our optimized protocol provides after one iteration a x and y -dependent concurrence. Although the numerically-obtained concurrence is larger at $x = 0$ and $y \in [-1, 1]$ than the surface given by Eq. (18), one can also observe the opposite at $y = 0$ and $x \in [-1, 1]$.

However, the concurrence presents a better improvement with our algorithm and the average cost function with the uniform PDF stays for more iterations lower than the CNOT-based protocol, see the left figure in panel 4. In regard to the overall success probability, we let our algorithm work until the third iteration and in Fig. 5 the results are compared with the CNOT-based purification protocol. The obtained surfaces differ only by a $\pi/2$ rotation around the z -axis. Therefore, there is not much difference in the overall success probability and from this aspect the CNOT gate can also be considered optimal, though, it still can not improve the concurrence as effectively as the gate obtained with our approach. However, one might think with a proper choice of local unitary transformations, like the transformation in Eq. (15) used for Werner and one-step purifiable states, the application of the CNOT gate may result in an optimal purification protocol. Let us consider then two general local unitary transformations at locations A and B for the preparation of two-qubit states. It is enough to consider unitary transformations in $SU(2)$, for which the Euler angle parameterization reads [27]

$$U_A = e^{i\sigma_z\alpha_1} e^{i\sigma_y\alpha_2} e^{i\sigma_z\alpha_3}, \quad (22)$$

$$U_B = e^{i\sigma_z\beta_1} e^{i\sigma_y\beta_2} e^{i\sigma_z\beta_3}, \quad (23)$$

where σ_y and σ_z are the Pauli matrices. Here, $\alpha_1, \beta_1 \in [0, \pi]$, $\alpha_2, \beta_2 \in [0, \pi/2]$, and $\alpha_3, \beta_3 \in [0, 2\pi]$ are the Euler angles for $SU(2)$. For the first iteration, we analyze the output unitary of the optimized protocol with *Mathematica* [28] and observe that the angles α_1 and β_1 do not affect the efficiency of the CNOT-based protocol. Optimal concurrences for the remaining four angles yield either the result in Eq. (18) or

$$\mathcal{C}'_{\text{CNOT}}(x, y) = \frac{2|y|}{1+y^2}, \quad (24)$$

with success probability

$$P_{\text{CNOT}} = \frac{1+y^2}{2}, \quad (25)$$

for $\alpha_2 = \frac{\pi}{8}$, $\beta_2 = \frac{3\pi}{8}$, and $\alpha_3 = \beta_3 = \frac{3\pi}{4}$. For these results the average cost function with uniform PDF yields $\bar{f} \approx 0.372$, which is still lower than the average concurrence found by our approach. These results demonstrate that even with local unitary transformations the CNOT gate is globally not optimal for all values of x and y . However, when x and y are known beforehand, then one can use the following local unitary transformation

$$U_A^\dagger \otimes U_B, \quad \text{with } U = \cos(\theta)\mathbb{I}_2 + \sin(\theta)\sigma_x, \quad (26)$$

where the angle θ is a function of x and y . For example,

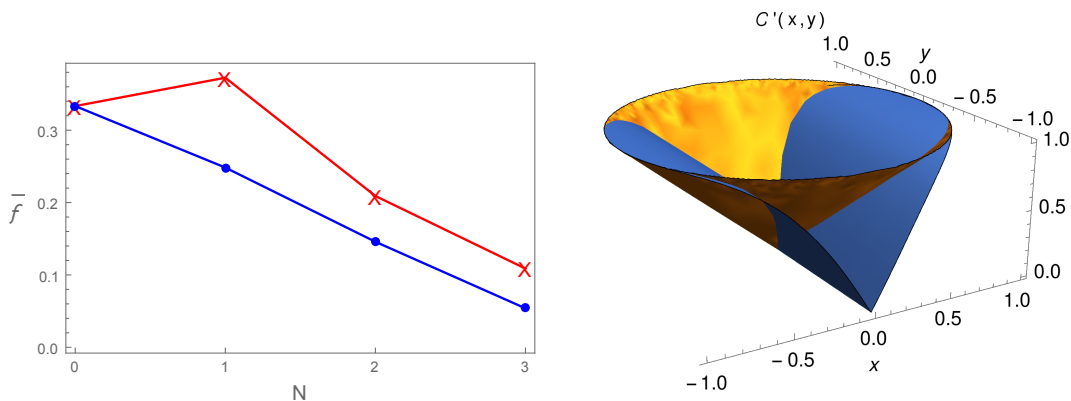


FIG. 4: Optimized purification protocol for the state in Eq. (17). Left panel: Average cost function \bar{f} with a uniform PDF as a function of N , the number of iterations. Crosses are the results of the CNOT gate, whereas dots display the numerical optimization. They have been connected by lines to guide the eye. Right panel: The concurrence C' as a function of x and y after one purification round. The cone-type surface is obtained with our approach. A less optimal surface with minima at $x = 0$ and along the y axis is the result of the purification protocol with the CNOT gate.

for $x, y \geq 0$, we have

$$\cos(\theta) = \sqrt{\frac{1}{2} + \frac{x + \sqrt{x^2 + y^2}}{8\sqrt{x^2 + y^2}}}.$$

Using this transformation before the purification protocol, one obtains the state

$$\frac{1 + \sqrt{x^2 + y^2}}{2} |\Psi^-\rangle \langle \Psi^-| + \frac{1 - \sqrt{x^2 + y^2}}{2} |\Phi^-\rangle \langle \Phi^-|. \quad (27)$$

Now, the CNOT-based purification yields

$$C'_{\text{CNOT}}(x, y) = \frac{2\sqrt{x^2 + y^2}}{1 + x^2 + y^2}, \quad (28)$$

with success probability

$$P_{\text{CNOT}} = \frac{1 + x^2 + y^2}{2}. \quad (29)$$

It is immediate that $C'_{\text{CNOT}}(x, y) \geq \sqrt{x^2 + y^2}$, i.e., we are improving the concurrence. In this particular case, one does not need the average cost function in the numerical search, because the state is fixed. Our algorithm running with a single state with parameters (x, y) as defined in Eq. (17) instead of an ensemble of states can improve the concurrence, but is unable to find the optimal solution presented above, because the transformation Eq. (26) together with CNOT gates is a non-symmetrical transformation at nodes A and B .

Finally, let us point out that our approach does not take into account operational or memory errors. These always depend on the implementation and if an experiment can provide us models for the errors then our ap-

proach can be easily extended. Another important experimental input is the PDF $p(\mathbf{x})$, which is usually subject to the method of generating entangled states between locations A and B . Furthermore, this PDF is assigned to the process of choosing a value \mathbf{x} as a random event, i.e., we have the same two two-qubit pairs parameterized by \mathbf{x} before the purification protocol. In effect, we integrate the parameter dependence of the states away and thus our approach yields an optimal two-qubit gate on average. If the value of \mathbf{x} is fixed in an experimental design, then our method provides an optimal two-qubit gate designed for this particular state. The optimal two-qubit gates can be realized by three CNOT gates and additional single-qubit rotations [29, 30], and therefore the experimental generation of this gate is possible with high fidelity [31]. Also in the context of trapped ions or superconducting quantum circuits, the generation of two-qubit entangling gates can be achieved with high precision using the Mølmer-Sørensen gate [32] or the \sqrt{i} SWAP [33] gate. Since two-qubit unitaries have a straightforward implementation in many physical settings, thanks to quantum compilation [34], we argue that quantum computing platforms implementing quantum communication could actually benefit from globally optimal gates for entanglement purification.

IV. CONCLUSIONS

In the context of entanglement purification and recurrence protocols, we have presented a method to obtain optimal protocols. This method searches for the optimal two-qubit gate, which is applied bilaterally at the nodes A and B in order to distill from an ensemble of noisy pairs a higher fidelity state with respect to a maxi-

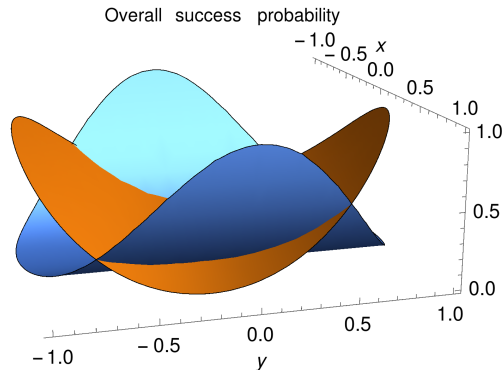


FIG. 5: The overall success probability of the state in Eq. (17) after and $N = 3$ iterations as a function of x and y . Both surfaces are similar in appearance. The one having maxima at $x = 1$ belongs to the CNOT-based protocol and the other one having maxima at $y = 1$ is obtained via the optimized numerical protocol.

mally entangled state. Our strategy considers situations, where the experimental apparatus does not have enough control over the entanglement generation phase and different experimental runs result in different states. Here, we assume that the same copies of the noisy state can be generated before the purification protocol takes place, but a different experimental run could result in different states. Errors originating from local operations, memory requirements, or even classical communication are neglected for now.

We have numerically demonstrated the optimality of our proposal for several states. In the case of the Werner state, we have found several optimal two-qubit gates and their performances are the same as the CNOT-based Bennett protocol [25]. Thus, for Werner states the optimality cannot be improved beyond the already known performance. Next, we have investigated a family of states that one can purify in one step, i.e., two noisy copies of states are enough to obtain a maximally entangled state, where we immediately obtain minimal average cost function $\bar{f} \approx 0$, as expected. Finally, we consider a two-parameter family of states which is considered in theoretical models of a quantum repeater [26]. Our numerical investigations demonstrate that a single bilaterally applied CNOT gate cannot be globally optimal for these states. On the other hand, when the state is known, then parameter-dependent, non-symmetric local transformations allow again the CNOT to be also one of the optimal two-qubit gates. This case exemplifies the difference between protocols that are optimal for a full class of parameterized states and those that are only optimal for a single state.

In conclusion, we have proposed a general method to optimize entanglement purification for an arbitrary family of states. Our algorithm [35] can find the most optimal two-qubit gate that on average induces the highest increase of entanglement. We remark that the method is general for the set of parameters defining the states. Optimizing for a single state is also possible, as shown in one of the presented examples. Furthermore, we have focused on the degree of entanglement measured by the concurrence and not on the fidelity with respect to a particular Bell state. This is motivated by the fact that there exist an infinite number of maximally entangled states, and therefore entangled mixed states can present a larger fidelity with respect to maximally entangled states that might not correspond to Bell states defined in the computational basis. A possible drawback is that one cannot know with certainty the final maximally entangled state produced by the protocol. This and other issues such as different input states, asymmetric two-qubit gates, and non-ideal local operations remain open questions. However, this work aims to introduce the concept of globally optimized recurrence protocols that is flexible enough to incorporate the aforementioned points in further investigations, which we plan to carry out in the future.

ACKNOWLEDGMENTS

This work is supported by the DFG under Germany's Excellence Strategy-Cluster of Excellence Matter and Light for Quantum Computing (ML4Q) EXC 2004/1-390534769. The results were obtained using the libraries JAX [19], Scipy [36] and QuTiP [37].

Appendix A: Gell-Mann type basis

In this Appendix, details concerning the Gell-Mann type basis for the Lie algebra of $SU(4)$ are shown. The matrices read

$$\begin{aligned}
\sigma_1 &= \begin{pmatrix} 0 & 1 & 0 & 0 \\ 1 & 0 & 0 & 0 \\ 0 & 0 & 0 & 0 \\ 0 & 0 & 0 & 0 \end{pmatrix}, & \sigma_2 &= \begin{pmatrix} 0 & -i & 0 & 0 \\ i & 0 & 0 & 0 \\ 0 & 0 & 0 & 0 \\ 0 & 0 & 0 & 0 \end{pmatrix}, & \sigma_3 &= \begin{pmatrix} 1 & 0 & 0 & 0 \\ 0 & -1 & 0 & 0 \\ 0 & 0 & 0 & 0 \\ 0 & 0 & 0 & 0 \end{pmatrix}, \\
\sigma_4 &= \begin{pmatrix} 0 & 0 & 1 & 0 \\ 0 & 0 & 0 & 0 \\ 1 & 0 & 0 & 0 \\ 0 & 0 & 0 & 0 \end{pmatrix}, & \sigma_5 &= \begin{pmatrix} 0 & 0 & -i & 0 \\ 0 & 0 & 0 & 0 \\ i & 0 & 0 & 0 \\ 0 & 0 & 0 & 0 \end{pmatrix}, & \sigma_6 &= \begin{pmatrix} 0 & 0 & 0 & 0 \\ 0 & 0 & 1 & 0 \\ 0 & 1 & 0 & 0 \\ 0 & 0 & 0 & 0 \end{pmatrix}, \\
\sigma_7 &= \begin{pmatrix} 0 & 0 & 0 & 0 \\ 0 & 0 & -i & 0 \\ 0 & i & 0 & 0 \\ 0 & 0 & 0 & 0 \end{pmatrix}, & \sigma_8 &= \frac{1}{\sqrt{3}} \begin{pmatrix} 1 & 0 & 0 & 0 \\ 0 & 1 & 0 & 0 \\ 0 & 0 & -2 & 0 \\ 0 & 0 & 0 & 0 \end{pmatrix}, & \sigma_9 &= \begin{pmatrix} 0 & 0 & 0 & 1 \\ 0 & 0 & 0 & 0 \\ 0 & 0 & 0 & 0 \\ 1 & 0 & 0 & 0 \end{pmatrix}, \\
\sigma_{10} &= \begin{pmatrix} 0 & 0 & 0 & -i \\ 0 & 0 & 0 & 0 \\ 0 & 0 & 0 & 0 \\ i & 0 & 0 & 0 \end{pmatrix}, & \sigma_{11} &= \begin{pmatrix} 0 & 0 & 0 & 0 \\ 0 & 0 & 0 & 1 \\ 0 & 0 & 0 & 0 \\ 0 & 1 & 0 & 0 \end{pmatrix}, & \sigma_{12} &= \begin{pmatrix} 0 & 0 & 0 & 0 \\ 0 & 0 & 0 & -i \\ 0 & 0 & 0 & 0 \\ 0 & i & 0 & 0 \end{pmatrix}, \\
\sigma_{13} &= \begin{pmatrix} 0 & 0 & 0 & 0 \\ 0 & 0 & 0 & 0 \\ 0 & 0 & 0 & 1 \\ 0 & 0 & 1 & 0 \end{pmatrix}, & \sigma_{14} &= \begin{pmatrix} 0 & 0 & 0 & 0 \\ 0 & 0 & 0 & 0 \\ 0 & 0 & 0 & -i \\ 0 & 0 & i & 0 \end{pmatrix}, & \sigma_{15} &= \frac{1}{\sqrt{6}} \begin{pmatrix} 1 & 0 & 0 & 0 \\ 0 & 1 & 0 & 0 \\ 0 & 0 & 1 & 0 \\ 0 & 0 & 0 & -3 \end{pmatrix}.
\end{aligned} \tag{A1}$$

Actually, these matrices together with the identity matrix

$$\sigma_0 = \begin{pmatrix} 1 & 0 & 0 & 0 \\ 0 & 1 & 0 & 0 \\ 0 & 0 & 1 & 0 \\ 0 & 0 & 0 & 1 \end{pmatrix}$$

form an orthogonal basis for the space $M_n(\mathbb{C})$ of 4×4 matrices with complex entries equipped with Hilbert-Schmidt scalar product

$$\langle A, B \rangle = \text{Tr}\{A^\dagger B\}, \quad A, B \in M_n(\mathbb{C}),$$

where A^\dagger is the adjoint of A . We first note that $\sigma_i^\dagger = \sigma_i$ for all $i \in \{0, 1, 2, \dots, 15\}$. Therefore, every matrix $X \in M_n(\mathbb{C})$ can be written as

$$X = \sum_{i=0}^{15} \frac{\langle \sigma_i, X \rangle}{\langle \sigma_i, \sigma_i \rangle} \sigma_i, \quad \text{and} \quad X^\dagger = \sum_{i=0}^{15} \frac{\langle \sigma_i, X \rangle^*}{\langle \sigma_i, \sigma_i \rangle} \sigma_i,$$

where z^* is the complex conjugate of the complex number $z \in \mathbb{C}$. In this fashion, one can obtain another representation for any element $U \in SU(4)$ fulfilling $U^\dagger U = U U^\dagger = \sigma_0$ and including also that its determinant equal to one. This is also a minimal parametrization, however, a cumbersome one compared to the Euler angle parametrization. In general, a Gell-Mann type basis for the Lie algebra of $SU(n)$ can always be obtained, see Refs. [27, 38].

[1] C. Monroe, W. C. Campbell, L.-M. Duan, Z.-X. Gong, A. V. Gorshkov, P. W. Hess, R. Islam, K. Kim, N. M. Linke, G. Pagano, P. Richerme, C. Senko, and N. Y. Yao, *Rev. Mod. Phys.* **93**, 025001 (2021).

[2] T. Albash and D. A. Lidar, *Rev. Mod. Phys.* **90**, 015002 (2018).

[3] S. Pirandola, U. L. Andersen, L. Banchi, M. Berta, D. Bunandar, and R. Colbeck, *et al.* *Adv. Opt. Photon.* **12**,

- 1012 (2020).
- [4] D. Awschalom, *et al.* PRX Quantum **2**, 017002 (2021).
- [5] Peres, Asher, "Reversible Logic and Quantum Computers". Physical Review A. **21**, 3266–3276 (1985).
- [6] Devitt, Simon J; Munro, William J; Nemoto, Kae. "Quantum error correction for beginners". Reports on Progress in Physics. **76**, 076001 (2013).
- [7] C. H. Bennett, G. Brassard, S. Popescu, B. Schumacher, J. A. Smolin, and W. K. Wootters, Phys. Rev. Lett. **76**, 722 (1996); **78**, 2031 (1997).
- [8] D. Deutsch, A. Ekert, R. Jozsa, C. Macchiavello, S. Popescu, and A. Sanpera, Phys. Rev. Lett. **77**, 2818 (1996); **80**, 2022 (1998).
- [9] C. H. Bennett, D. P. DiVincenzo, J. A. Smolin, and W. K. Wootters, Phys. Rev. A **54**, 3824 (1996).
- [10] W. Dür and H. J. Briegel, Rep. Prog. Phys. **70**, 1381 (2007).
- [11] S. Krastanov, V. V. Albert, and L. Jiang, Quantum **3**, 123 (2019).
- [12] R. F. Werner, Phys. Rev. A **40**, 4277 (1989).
- [13] J. M. Torres and J. Z. Bernád, Phys. Rev. A **94**, 052329 (2016).
- [14] W. K. Wootters. Phys. Rev. Lett., **80**, 2245 (1998).
- [15] C.T. Kelley, *Iterative methods for optimization*, Frontiers in Appl. Math., **18**, SIAM (1999).
- [16] J. Z. Bernád, J. M. Torres, L. Kunz, and G. Alber, Phys. Rev. A **93**, 032317 (2016).
- [17] A. Baker, *Matrix Groups: An Introduction to Lie Group Theory* (Springer, London, 2002).
- [18] T. Tilma, M. Byrd, and E. C. G. Sudarshan, J. Phys. A: Math. Gen. **35**, 10445 (2002).
- [19] J. Bradbury, R. Frostig, P. Hawkins, M. J. Johnson, C. Leary, D. Maclaurin, G. Necula, A. Paszke, J. VanderPlas, S. Wanderman-Milne, and Q. Zhang, JAX: composable transformations of Python+NumPy programs, <http://github.com/google/jax> (2018).
- [20] D.C. Liu and J. Nocedal, Mathematical Programming **45**, 503 (1989).
- [21] R. H. Byrd, P. H. Lu, J. Nocedal, C. Y. Zhu, SIAM J. Sci. Comput., **16**, 1190 (1995).
- [22] G. Kimura, Phys. Lett. A **314**, 339 (2003).
- [23] M. S. Byrd and N. Khaneja, Phys. Rev. A **68**, 062322 (2003).
- [24] O. Gamel, Phys. Rev. A **93**, 062320 (2016).
- [25] C. H. Bennett, G. Brassard, S. Popescu, B. Schumacher, J. A. Smolin, and W. K. Wootters, Phys. Rev. Lett. **76**, 722 (1996); **78**, 2031 (1997).
- [26] J. Z. Bernád, Phys. Rev. A **96**, 052329 (2017); **97**, 069903(E) (2018).
- [27] T. Tilma and E. C. G. Sudarshan, J. Phys. A: Math. Gen. **35**, 10467 (2002).
- [28] See, <https://www.wolfram.com>.
- [29] G. Vidal and C. M. Dawson, Phys. Rev. A **69**, 010301(R) (2004).
- [30] F. Vatan and C. Williams, Phys. Rev. A **69**, 032315 (2004).
- [31] S. Debnath, N. M. Linke, C. Figgatt, K. A. Landsman, K. Wright, and C. Monroe, Nature **536**, 63 (2016).
- [32] A. Sørensen and K. Mølmer, Phys. Rev. Lett. **82**, 1971 (1999).
- [33] H. Fan, V. Roychowdhury, and T. Szkopek, Phys. Rev. A **72**, 052323 (2005).
- [34] E. A. Martinez, T. Monz, D. Nigg, P. Schindler, and R. Blatt, New J. Phys. **18**, 063029 (2016).
- [35] F. Preti, <https://github.com/franz3105/OptEntDist>.
- [36] P. Virtanen, R. Gommers, T. E. Oliphant, M. Haberland, T. Reddy, D. Cournapeau, E. Burovski, P. Peterson, W. Weckesser, J. Bright, S. J. van der Walt, M. Brett, J. Wilson, K. J. Millman, N. Mayorov, A. R. J. Nelson, E. Jones, R. Kern, E. Larson, C. J. Carey, I. Polat, Y. Feng, E. W. Moore, J. VanderPlas, D. Laxalde, J. Perktold, R. Cimrman, I. Henriksen, E. A. Quintero, C. R. Harris, A. M. Archibald, A. H. Ribeiro, F. Pedregosa, P. van Mulbregt, and SciPy 1.0 Contributors, Nat. Methods **17**, 261 (2020).
- [37] J. R. Johansson, P. D. Nation, and F. Nori, Comp. Phys. Comm. **184**, 1234 (2013).
- [38] S. Bertini, S. L. Cacciatori, and B. L. Cerchiai, J. Math. Phys. **47**, 043510 (2006).